Structural and Mechanical Properties of ZrSiN Thin Films Prepared by Reactive Magnetron Sputtering

F.G.R. Freitas[1, a], A.G.S. Conceição[1, b], R. Hübler[2, c], G. Soares[3, d], E.R. Vitória[1, b], R.G. Carvalho[1, b] and E.K. Tentardini[1, b]

[1]Universidade Federal de Sergipe, Av. Marechal Rondon, s/n – São Cristóvão – Brazil

[2]Pontifícia Universidade Católica do Rio Grande do Sul, Av. Ipiranga, 6681 – Porto Alegre – Brazil

[3]Universidade Federal do Rio Grande do Sul, Av. Paulo Gama, 110 – Porto Alegre – Brazil

[a]flaviogus@hotmail.com, [b]etentardini@gmail.com, [c]hubler@pucrs.br, [d]gabriel.soares@ufrgs.br

Keywords: Thin films, ZrSiN, magnetron sputtering, nanohardness, RBS.

Abstract. Zirconium silicon nitride (ZrSiN) thin films were deposited by reactive magnetron sputtering in order to verify the silicon influence on coating morphology and mechanical properties. The Si/(Zr+Si) ratio was adjusted between 0 to 14.5% just modifying the power applied on the silicon target. Only peaks associated to ZrN crystalline structure were observed in XRD analysis, since Si_3N_4 phase was amorphous. All samples have (111) preferred orientation, but there is a peak intensity reduction and a broadening increase for the sample with the highest Si/(Zr+Si) ratio (14.5%), demonstrating a considerable loss of crystallinity or grain size reduction (about 8 nm calculated by Scherrer). It was also observed that the texture coefficient for (200) increases with silicon addition. Chemical composition and thickness of the coatings were determined by RBS analysis. No significant changes in nanohardness with increasing Si content were found. The thin film morphology observed by SEM presents columnar and non columnar characteristics. The set of results suggests that Si addition is restricting the columnar growth of ZrN thin films. This conclusion is justified by the fact that Si contributes to increase the ZrN grains nucleation during the sputtering process.

Introduction

Nitride transition metal thin films have been used in the last decades due to properties as hardness, wear resistance, mechanical strength, etc. [1-3]. Zirconium nitride (ZrN) is a typical coating used because of its tribological properties and corrosion and oxidation resistance. Even with differentiated properties, ZrN thin films have columnar microstructure, micro-cracks and pores, which are defects associated with reactive magnetron sputtering deposition process characteristics. These discontinuities allow direct contact between the external environment and the substrate, compromising the mechanical properties and applications in high temperature or corrosive environments [4-6].

An alternative to modify ZrN thin films microstructure and morphology is the addition of a third element as silicon. The Si addition promotes the formation of a two phase microstructure, which one is crystalline (ZrN) and the other is amorphous (Si_3N_4). The amorphous phase is located at the grain boundaries and contributes to reduce the ZrN grain size, since it increases the ZrN grains nucleation rate. The final grain size is less than 10 nm, resulting in the formation of a nanocomposite structure. These characteristics have potential to change thin film morphology and macroscopic properties [7-9].

The study proposal was to deposit thin films of ZrSiN system by reactive magnetron sputtering varying the Si concentration in each coating. XRD, SEM, RBS and nanohardness techniques were used to analyze the morphology and mechanical properties of the coatings.

Materials and Methods

The thin films used in this work were deposited by reactive magnetron sputtering with an AJA Orion 5-HV Sputtering Systems model with a deposition rate sensor coupled. Before deposition, the specimens were underwent ultrasonic cleaning in acetone during 30 minutes, washed with alcohol and then dried. The chamber was preconditioned to a base pressure of $1x10^{-7}$ Torr and targets were bombarded ionically to remove oxide layers from the surface before deposition.

All deposition parameters were maintained constant during depositions except the power used at silicon target, as showed in Table 1. Different substrates were used according to the characterization technique: silicon wafer for XRD, nanohardness and SEM analysis and polyethylene plates for RBS studies. The thickness was also adjusted to comply with the required analysis, 50 nm for RBS, 300 nm for SEM and XRD and 600 nm for nanohardness.

Table 1 – Sputtering deposition parameters.

Sample	Working Pressure [mTorr]	Zr DC Power [W/cm²]	Si RF Power [W/cm²]	N_2+Ar flux [sccm]	Temperature [°C]
ZrN	3.0	6.0	0.0	21.0	30.0
ZrSiN_1	3.0	6.0	1.2	21.0	30.0
ZrSiN_2	3.0	6.0	2.2	21.0	30.0
ZrSiN_3	3.0	6.0	3.7	21.0	30.0

The XRD diffractions were performed on a Shimadzu XRD-6000 model with grazing angle of 1° (Cu-Kα radiation – λ = 1.54 Å). The morphology of the film cross section was observed on a high-resolution FEG-SEM JSM-6330F with an EDS system coupled.

Nanohardness analysis were performed in a Fisherscope HV 100 with a Berkovich indenter and indentation depth of 40 nm. This technique also permits to determine the films Young's modulus. RBS analysis were performed using a 3 MV tandetron with alpha particles accelerated up to 2 MeV, with a silicon based detector at an angle of 165° and resolution of 12 keV.

Results and Discussion

The stoichiometric ZrN film has a metallic gold color [10] and the ZrN coating deposited with Ar/N_2 ratio of 19/2 presented this characteristic. A set of ZrSiN thin films modifying Si concentration were deposited using different powers applied on the silicon target. These samples were analyzed by RBS technique to measure coatings thickness, identify chemical elements and the respective concentration of each one. All samples present similar results, except the silicon peak, which is function of the power applied to the Si target. For this reason it is presented only the spectra for sample ZrSiN_3 in Fig. 1.

Analyzing Fig. 1 is possible to identify the occurrence of Hf, Zr, Si, N and O from thin film and C from substrate. These chemical elements were detected for all samples. The hafnium presence is due to the contamination of this chemical element on Zr target, once by manufacturer data the target is 99.7% Zr and 0.3% Hf. RBS results also show that the films are near the stoichiometric concentration, confirming the Ar/N_2 ratio of 19/2.

Table 2 shows Zr, N and Si concentration in at% and Si/(Zr+Si) ratio for each coatings. The coatings Si/(Zr+Si) ratio were characterized as low (6%), intermediary (8%) and high (14%), respectively for sample ZrSiN_1, ZrSiN_2 and ZrSiN_3. The coatings thickness was estimated in approximately 60 nm for all samples.

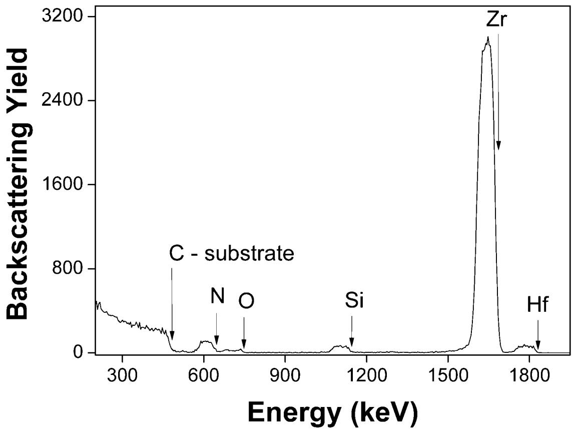

Figure 1: RBS analysis for sample ZrSiN_3. RBS confirmed the deposition of stoichiometric thin films of ZrSiN.

Table 2 – RBS analysis to N, Zr and Si concentrations and thickness.

Sample	N [at. %]	Zr [at. %]	Si [at. %]	Si / (Zr+Si) [%]	Thickness [nm]
ZrN	48.47	51.53	0.00	0.00	56.76
ZrSiN_1	48.36	48.43	3.21	6.22	58.96
ZrSiN_2	49.40	46.53	4.06	8.03	58.36
ZrSiN_3	45.86	46.31	7.83	14.47	64.39

Fig. 2a shows the XRD analysis for all samples. The ZrN, ZrSiN_1 and ZrSiN_2 XRD spectrum are almost identical, but the ZrSiN_3 has a peak intensity reduction and a small increase in (111) peak width, demonstrating a considerable loss of crystallinity or grain size reduction. Si_3N_4 structure is amorphous (confirmed by XRD) and its presence causes the reduction o the diffraction peaks intensity. Si_3N_4 particles contribute to ZrN grain nucleation process during film growth, resulting in a structure with reduced grain size [11,12]. The crystallite size calculated by Scherrer for ZrSiN_3 is about 8 nm (nanocomposite structure), while for others films is 11 nm. XRD small peaks at 54° for all samples are probably associated with ZrO_2 or $ZrSiO_4$ phases.

(a)

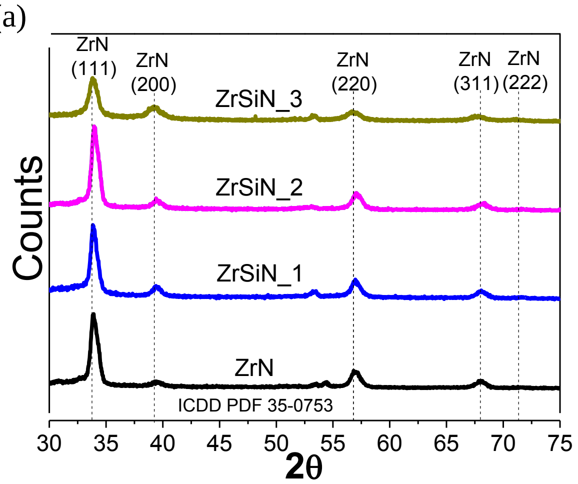

(b)

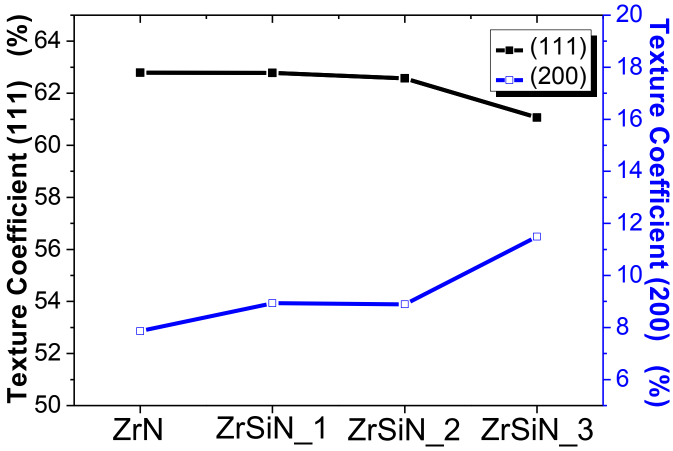

Figure 2(a) XRD analysis – (111) peak intensity reduction and broadening for ZrSiN_3 sample; 2(b) Preferred orientation – I(200)/I(111) ratio increase for ZrSiN_3 sample.

XRD analysis shows that ZrN film has strong (111) preferential orientation, but it can be observed at Fig. 2b that I(200)/I(111) ratio is increased with Si addition from 14.2% to 18.9%. Grains with (200) orientation have the lowest surface energy, while (111) have the lowest deformation energy. Thin films deposited by sputtering have high defects concentration, which causes crystal lattice distortion and promotes the (111) texture due to residual stress minimization [13,14]. (111) oriented grains grow in the normal direction to the film plane, which contributes to the formation of a columnar microstructure, while (200) grains grow in the parallel direction, having the potential to change the columnar morphology to a non columnar one [15].

Si addition act as a nucleation center for ZrN grains, reducing the crystallite size and creating thermodynamic conditions to the (200) oriented grains. The (200) indicates that the system is minimizing the surface energy and it can be concluded that the amount of defects in the film is reduced, which can improve thin film properties and characteristics.

Fig 3a shows nanohardness results. The ZrN hardness was about 15.6 GPa, value consistent with literature. Samples ZrSiN_1 and ZrSiN_2 had no significant variation in nanohardness (Si addition in low concentration was not enough to change the structure and mechanical properties). The ZrSiN_3 sample has the same hardness value, even with the crystallite size reduction. In this case, it can be noticed that this film has the highest I(200)/I(111) ratio, which means that the amount of defects were reduced, what contributes to nanohardness reduction. On the other hand, the ZrSiN_3 film has the lowest crystallite size and the microstructure is composed by ZrN and Si_3N_4 phases, effects that contribute to increase the nanohardness [16]. The global result is not having a significant impact in nanohardness properties.

Young's modulus results (Fig. 3a) has similar trend as observed for hardness values and the same interpretations can be pointed out for this material propertie.

SEM analysis (Fig. 3b) of thin films cross section shows a mixture of columnar morphology, which is a sputtering films characteristics, and non columnar regions. All ZrSiN coatings presented this same behavior. It can be verified that the Si addition promoted a transition from a columnar morphology to a non columnar one as the Si content is increased. This microstructure is aligned with XRD results, confirming the Si addition effect in changing the thin film morphology by blocking the columnar structure (Si restricts the columnar growth due to an increase in ZrN grain nucleation, which inhibits the (111) orientation and favors the (200) orientation).

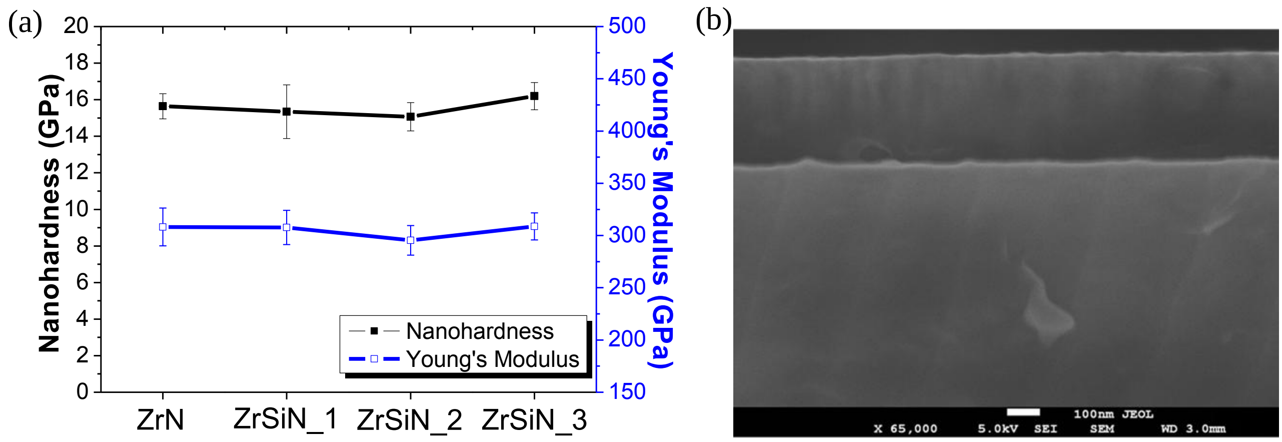

Figure 3(a) Nanohardness and Young's Modulus – it is verified no significant change for all films deposited; 3(b) SEM image for ZrSiN_2 – it can be observed a morphology composed of columnar and non columnar regions.

It can be verified that the thin films observed by SEM are homogeneous and have apparently good adhesion.

Conclusions

ZrN and ZrSiN were successively deposited by reactive magnetron sputtering. RBS analysis show ZrN coatings with stoichiometric near to 1:1 and the Si/(Zr+Si) ratio of ZrSiN coatings were determined as 6.2%, 8.0% and 14.5% when applied 1.2, 2.2 and 3.7 W/cm² at Si target, respectively. All coatings presented hafnium originated from zirconium target.

XRD analysis demonstrate that Si highest content film has a (111) peak broadening and intensity reduction, but the preferred orientation (111) is maintained. The crystallite size calculated by Scherrer pointed out that the Si effect creates a nanocomposite structure.

All films present strong (111) preferential orientation, but as the Si content is increased, it is observed an increase in I(200)/I(111) ratio. Si addition creates thermodynamic conditions to deposit (200) oriented grains, which causes a reduction in films defects concentration.

Nanohardness analysis indicated no significant modification in hardness with Si addition at ZrN coatings. Despite this, it was analyzed that the highest Si content sample has a set of characteristics that justifies the maintainability of its nanohardness (I(200)/I(111) ratio increase, crystallite size reduction and new microstructure composed by two phases). Young's modulus have the same behaviour as nanohardness.

SEM analysis show that ZrSiN thin films have both columnar and non columnar structure. Si addition blocks the columnar growth due to the favorable conditions to (200) orientation. Increasing the Si content in ZrN thin films, promotes a transition from a columnar structure to a non columnar one. It was also observed that ZrSiN thin films are homogeneous and have good adhesion.

References

[1] J. Musil., Hard and superhard nanocomposite coatings, Surface & Coatings Technology, 125 (2000) 322-330.

[2] M. Benkahoul, C.S. Sandu, N. Tabet, M. Parlinska-Wojtan, A. Karimi, F. Lévy, Effect of Si incorporation on the properties of niobium nitride films deposited by DC reactive magnetron sputtering, Surface & Coatings Technology, 188-189 (2004) 435-439.

[3] S. Veprek, M.G.J. Veprek-Heijman, Industrial applications of superhard nanocomposite coatings, Surface & Coatings Technology, 202 (2008) 5063-5073.

[4] G. Abadias, A. Michel, C. Tromas, C. Jaouen, S.N. Dub, Stress, interfacial effects and mechanical properties of nanoscale multilayered coatings, Surface and Coating Technology, 202 (2007) 844-853.

[5] J. Lee, G. Yang, Preparation of TiAlN/ZrN and TiCrN/ZrN multilayers by RF magnetron sputtering, Transactions of Nonferrous Metals Society of China, 19 (2009) 795-799.

[6] S. Ma, J. Prochazka, P. Karvankova, Q. Ma, X. Niu, X. Wang, D. Ma, K. Xu, S. Veprek, Comparative study of the tribological behavior of superhard nanocomposite coatings nc-TiN/a-Si3N4 with TiN, Surface & Coatings Technology, 194 (2005) 143-148.

[7] C.S. Sandu, R. Sanjinés, F. Medjani, Control of morphology (ZrN crystallite size and SiNx layer thickness) in Zr–Si–N nanocomposite thin films, Surface & Coatings Technology, 202 (2008) 2278-2781.

[8] D. Pilloud, J.F. Pierson, J. Takadoum, Structure ans tribological properties of reactively Zr-Si-N films, Thin Solid Films, 496 (2006) 445-449.

[9] C.S. Sandu, S. Harada, R. Sanjinés, A. Cavaleiro, A unique approach to reveal the nanocomposite nc-MN/SiN-layer architecture of thin films via electrical measurements, Surface & Coatings Technology, 204 (2010) 1907-1913.

[10] R. Lamni, E. Martinez, S.G. Springer, R. Sanjines, P.E. Schmid, F. Levy, Optical and electronic properties of magnetron sputtered ZrNx thin films, Thin Solid Films, 447-448 (2004) 316-321.

[11] J. Musil, Hard nanocomposite coatings: Thermal stability, oxidation resistance and toughness, Surface & Coatings Technology, 207 (2012) 50-65.

[12] C.S. Sandu, R. Sanjinés, F. Medjani, Control of morphology (ZrN crystallite size and SiNx layer thickness) in Zr–Si–N nanocomposite thin films, Surface & Coatings Technology, 202 (2008) 2278-2781.

[13] G. Abadias, Stress and preferred orientation in nitride-based PVD coatings, Surface and Coatings Technology, 202 (2008) 2223-2235.

[14] I. Goldfarb, J. Pelleg, L. Zevin, N. Croitoru, Lattice distortion in thin films of IVB metal (Ti, Zr, Hf) Nitrides, Thin Solid Films, 200 (1991) 117-127.

[15] R. Nanerjee, R. Chandra, P. Ayyub, Influence of the sputtering gas on the preferred orientation of nanocrystalline titanium nitride thin films, Thin Solid Films, 405 (2002) 64-72.

[16] J. Procházka, P. Karvánková, M.G.J. Veprek-Heijman, S. Veprek, Conditions required for achieving superhardness of ≥ 45 GPa in nc-TiN/a-Si3N4 nanocomposites, Materials Science & Engineering A, 384 (2004) 102-116.